NIH Public Access
Author Manuscript
*J Cell Sci*. Author manuscript; available in PMC 2009 September 1.

Published in final edited form as:
*J Cell Sci*. 2008 September 1; 121(Pt 17): 2871–2879. doi:10.1242/jcs.023705.

# TRPV4 enhances cellular uptake of aminoglycoside antibiotics

**Takatoshi Karasawa**[1], **Qi Wang**[1], **Yi Fu**[2,3], **David M. Cohen**[2,3], and **Peter S. Steyger**[1]

[1]Oregon Hearing Research Center, Portland, OR 97239, USA

[2]Division of Nephrology and Hypertension, Oregon Health & Science University, Portland, OR 97239, USA

[3]Portland Veterans Affairs Medical Center, Portland, OR 97239, USA

## Summary

The cochlea and kidney are susceptible to aminoglycoside-induced toxicity. The non-selective cation channel TRPV4 is expressed in kidney distal tubule cells, and hair cells and the stria vascularis in the inner ear. To determine if TRPV4 is involved in aminoglycoside trafficking, we developed a murine proximal tubule cell line KPT2 and a distal tubule cell line KDT3. TRPV4 expression was confirmed in KDT3 cells but not in KPT2 cells. Removal of extracellular $Ca^{2+}$ significantly enhanced gentamicin-Texas Red (GTTR) uptake by KDT3, indicative of drug uptake by non-selective cation channel permeation. To determine if TRPV4 is permeable to GTTR, stable cell lines were generated that express TRPV4 in KPT2 (KPT2-TRPV4). KPT2-TRPV4 cells took up more GTTR than control cell lines (KPT2-pBabe) in the absence of extracellular $Ca^{2+}$. TRPV4-dependent GTTR uptake was abolished by a point mutation within the critical channel pore region, suggesting that GTTR permeates the TRPV4 channel. In an endolymph-like extracellular environment, clearance of GTTR was attenuated from KPT2-TRPV4 cells in a TRPV4-dependent fashion. We propose that TRPV4 may play a role in aminoglycoside uptake and retention in the cochlea.

### Keywords

gentamicin; ototoxicity; aminoglycosides; cochlea; hair cells; stria vascularis; TRPV4; drug permeability

## Introduction

Aminoglycoside antibiotics are clinically important drugs and frequently used worldwide (Forge and Schacht, 2000). Aminoglycosides are highly effective in treating life-threatening Gram-negative bacterial infections, such as meningitis and bacterial sepsis in infants (Klein, 1984; Grohskopf et al., 2005). Drug entry into bacteria is energy-dependent. Active export of cations out of the cytosol hyperpolarizes bacteria, and induces an electrophoretic driving force that promotes the entry of cationic aminoglycosides. A pH gradient between acidic extra-bacterial fluids compared to the more alkaline cytosolic environments of bacteria also contributes to aminoglycoside entry (Taber et al., 1987). In bacteria, aminoglycosides bind to ribosomal RNA and induce mistranslation and inhibition of protein synthesis, resulting in bacterial death (Davies and Davis, 1968; Noller, 1991).

*Correspondence should be addressed to: P.S. Steyger, Ph.D. Oregon Hearing Research Center Oregon Health & Science University 3181 Sam Jackson Park Road Portland, OR 97239 USA FAX: (+1) 503-494-5656 Voice: (+1) 503-494-1062 E-mail: steygerp@ohsu.edu.

NIH-PA Author Manuscript
NIH-PA Author Manuscript
NIH-PA Author Manuscript

NIH-PA Author Manuscript

NIH-PA Author Manuscript

NIH-PA Author Manuscript

Therapeutic use of aminoglycosides is problematic, because these drugs are also nephrotoxic and ototoxic. Aminoglycoside-induced nephrotoxicity results in increased morbidity during and after treatment, and can cause kidney failure. Acute renal toxicity is largely reversible because kidney tubule cells can proliferate and replace cells lost to aminoglycoside toxicity (Mingeot-Leclercq and Tulkens, 1999). However, ototoxicity is mostly permanent because mammalian inner ear sensory hair cells do not regenerate following aminoglycoside-induced cytotoxicity (Chen et al., 1999; Lowenheim et al., 1999).

Aminoglycoside toxicity occurs via cell death mechanisms that include activation of caspase-3 and -9, reactive oxygen species formation, and the c-jun N-terminal kinases (JNKs) activation (Lee et al., 2004; Hirose et al., 1997; Pirvola et al., 2000). Since it is difficult to inhibit the variety of cell death mechanisms that may be induced by aminoglycosides, another strategy to prevent aminoglycoside-induced ototoxicity is to block the drug entry into cells. To identify pharmacological blockers for aminoglycoside entry, it is important to understand how cells take up aminoglycosides.

One mechanism by which inner ear hair cells take up aminoglycosides is endocytosis at the apical membrane (Hashino and Shero, 1995; Hiel et al., 1992). Internalized aminoglycosides are transported into lysosomes, where the drugs accumulate over time and disrupt lysosomes (Hashino et al., 1997). In kidney cells, aminoglycosides are also transported through Golgi complex and the endoplasmic reticulum (ER) in a retrograde manner, and subsequently released into the cytosol from the ER (Sandoval and Molitoris, 2004).

There is another mechanism of aminoglycoside entry, which is ion channel permeation into cells. In cochlear sensory hair cells, aminoglycosides permeate through the mechanosensitive transduction channels located at the tips of individual stereocilia comprising the hair bundle (Marcotti et al., 2005). In cultured kidney cells, chemical agonists of the TRPV1 channel, low extracellular $Ca^{2+}$ levels, warm temperatures, negative cellular potentials or acidic extracellular pH enhance rapid cellular uptake of aminoglycosides, suggestive of ion channel permeation (Myrdal and Steyger, 2005; Meyers et al., 2003).

Endocytosis is temperature-dependent in euthermic birds and mammals (37-38°C) and slows down at hypothermic temperatures (Mamdouh et al., 1996). However, rapid aminoglycoside uptake and toxicity occurs at room temperature and 4°C in vitro (Myrdal et al., 2005; Myrdal and Steyger, 2005; Hirose et al., 1997), further supporting aminoglycoside permeation through non-selective cation channels. This likely involves Transient Receptor Potential (TRP) channels including TRPV1, as regulators of these channels modulate aminoglycoside uptake (Myrdal and Steyger, 2005).

In the kidney, proximal tubule cells are more sensitive to aminoglycoside-induced cytotoxicity, presumably because these cells take up and retain the drugs. On the other hand, distal tubule cells are more resistant to aminoglycosides, most likely because these cells do not retain aminoglycosides in the cytoplasm. One major difference between proximal and distal tubule cells is TRPV4, another TRP channel, which is abundantly expressed in distal tubule cells but not in proximal tubule cells (Strotmann et al., 2000; Tian et al., 2004). TRPV4 is a mechanosensitive receptor that is responsive to systemic osmotic pressure induced by cell swelling in hypo-osmotic media (Liedtke et al., 2000; Strotmann et al., 2000). In the kidney, TRPV4 is only expressed in water-impermeant nephron segments and where generation of a substantial osmotic gradient could be expected (Tian et al., 2004). In the cochlea, TRPV4 is expressed in hair cells and the stria vascularis (Liedtke et al., 2000; Takumida et al., 2005; Shen et al., 2006). In this study, we characterize TRPV4 expression in the inner ear and kidney, and determine that TRPV4 can mediate aminoglycoside uptake

NIH-PA Author Manuscript

NIH-PA Author Manuscript

NIH-PA Author Manuscript

and retention using kidney cell lines. Our data lead us to propose that TRPV4 channels may be involved in aminoglycoside uptake and retention in the inner ear.

## Results

### TRPV4 expression in kidney and inner ear

To determine if TRPV4 is appropriately located to contribute to aminoglycoside trafficking in the kidney and inner ear, the protein expression of TRPV4 was characterized by immunofluorescence in these tissues. In Madin-Darby canine kidney (MDCK) cells, TRPV4 protein was preferentially localized at the basolateral membrane (Fig. 1A), consistent with known expression pattern of TRPV4 in kidney (Tian et al., 2004). TRPV4 was also detected in the basolateral membranes of murine kidney distal tubule cells (Fig. 1B), but not in adjacent tubular segments, nor in the kidney of TRPV4-deficient mice (Fig. 1C). In the inner ear, TRPV4 immunoexpression was observed in the stria vascularis and organ of Corti as reported previously (Liedtke et al., 2000;Takumida et al., 2005). In the stria vascularis, TRPV4 was localized at the lumenal surface of marginal cells (Fig. 1D,E,P,Q), and only weakly within their somata (Fig. 1G,H,P,Q). TRPV4 was preferentially localized in intermediate cells (Fig. 1G,H,J,K,M,N,P,Q), which surround the entire basolateral membrane of marginal cells, interdigitating between marginal cells separating them from another, as previously described (Takeuchi et al., 2001). TRPV4 was not detected in the stria vascularis of TRPV4-deficient mice (Fig. 1F,I,L,O).

In the organ of Corti of wild-type mice, TRPV4 expression was most prominent in the region of tight junctions between adjacent pillar cells, and also between adjacent Deiters' cell phalanges (Fig. 1R,S). The stereocilia of inner hair cells displayed a distinct TRPV4 expression pattern (Fig. 1R,S) in contrast to the outer hair cell (OHC) stereocilia, which showed much weaker TRPV4 expression (data not shown). TRPV4 expression was also localized in Deiters' cell phalanges, and weakly in OHC bodies and spiral ganglion cells (Fig. 1R,T). TRPV4 expression was not detected in organ of Corti of TRPV4-deficient mice (data not shown).

### Murine kidney cell line generation and TRPV4 expression analysis

To compare aminoglycoside uptake between kidney proximal and distal tubule cells, we obtained spontaneously immortalized proximal and distal tubule cell lines from murine kidney. Primary kidney cell cultures were maintained for three to four weeks. Out of thirty growing cell colonies that were subcultured, three clones became immortalized. Two cell lines looked alike, with a fibroblast-like morphology, and a third appeared more epitheloid, with a classic epithelial/cobblestone appearance and smooth edges to cell clusters (Fig. 2A,B). This morphological difference was also reflected in TRPV4 expression levels revealed by RT-PCR and immunoblotting (Fig. 2C,D). Although RT-PCR detected TRPV4 transcript in all three cell lines at the expected size (410 bp), the third, epitheloid cell line had a significantly higher level than the other two (Fig. 2C). The control β-actin band (373 bp), however, showed a lower level of expression in the third cell line compared to the other two (Fig. 2C). In immunoblots, two TRPV4 bands around 110 kDa were detected in the epitheloid cell line, with the upper one being possible doublet bands (Fig. 2D). This is consistent with previous reports that the upper bands are the glycosylated and/or phosphorylated forms (Xu et al., 2003). Similar to the RT-PCR data, the epitheloid cell line showed actin protein (42 kDa) at a lower level than the other two cell lines (Fig. 2D). Although the actin antibody detects all the major actin isoforms including α-, β-, and γ-actin, the differences in β-actin levels are likely reflected in the immunoblot. The higher actin expression levels in the first two cell lines possibly originated from high actin expression in brush border of kidney proximal tubule. Using confocal microscopy, TRPV4 was

NIH-PA Author Manuscript

NIH-PA Author Manuscript

NIH-PA Author Manuscript

prominently localized at the basolateral membrane of the third cell line with low apical membrane expression (Fig. 2F,G), but not in the other two cell lines (Fig. 2E). Based on both morphology and TRPV4 expression, two cell lines appeared to be proximal tubule cells, while the third TRPV4-expressing cell line was derived from the distal tubule or collecting duct. We designated these cell lines KPT1, KPT2, and KDT3, respectively.

## GTTR uptake in kidney cells is enhanced in the absence of extracellular $Ca^{2+}$

A fluorescent conjugate of gentamicin and Texas Red (GTTR) is useful to study non-endocytotic aminoglycoside uptake in cells, and its intracellular localization (Myrdal et al., 2005; Myrdal and Steyger, 2005). KPT2 and KDT3 cells were treated with 5 μg/ml GTTR for 30 seconds at room temperature to determine their comparative rate of GTTR uptake. In the presence of physiological 1.25 mM extracellular $Ca^{2+}$, there were low levels of GTTR fluorescence within KPT2 and KDT3 cells, although significantly more GTTR fluorescence was observed in KPT2 cells compared to KDT3 cells (Fig. 3A,B). The intensity of cytoplasmic GTTR fluorescence in KDT3 cells was only 62% of that in KPT2 cells in the presence of extracellular $Ca^{2+}$ (Fig. 3E). Incubation of cells with GTTR in the absence of extracellular $Ca^{2+}$ substantially increased GTTR fluorescence in both cell types (Fig. 3C,D,E, $p<0.001$ between 1.25 mM and 0 mM $Ca^{2+}$ for both KPT2 and KDT3). This increase was significantly greater (2.2 fold) in KDT3 cells compared to the 1.5-fold increase in KPT2 cells, resulting in similar uptake levels (Fig. 3C,D,E). In both KPT2 and KDT3 cells, GTTR fluorescence was diffusely distributed in the cytoplasm, with a small punctate pattern within the nucleus, reminiscent of the GTTR-labeled nucleoli described in Opossum Kidney (OK) and MDCK cells (Myrdal et al., 2005).

These results suggest that aminoglycoside uptake in KDT3 cells is very sensitive to extracellular $Ca^{2+}$ levels, while uptake in KPT2 cells is also affected by extracellular $Ca^{2+}$. Removal of extracellular $Ca^{2+}$ increases inward currents of TRPV4 channels (Voets et al., 2002). It is possible that TRPV4 is a major determinant in aminoglycoside uptake in KDT3 cells, and the GTTR uptake difference in the presence of extracellular $Ca^{2+}$ is due to a reduced inward current by TRPV4 in KDT3 cells. The GTTR uptake enhancement in KPT2 cells by extracellular $Ca^{2+}$ removal suggests that these cells express other calcium-sensitive cation channels, which are also permeable to GTTR.

## GTTR uptake is enhanced by TRPV4 in the absence of extracellular $Ca^{2+}$

To test if TRPV4 channel enhances GTTR uptake, stable cell lines that express TRPV4 were generated using KPT2 cells. Three KPT2-derived, exogenous TRPV4-expressing cell lines (KPT2-TRPV4) and three vector control cell lines (KPT2-pBabe) were generated, all of which retained parental KPT2 morphology. Immunoblotting and immunofluorescence confirmed TRPV4 expression in all KPT2-TRPV4 and negligible TRPV4 expression in KPT2-pBabe cells (Fig. 4A-D). Unlike KDT3 cells, the upper band in these KPT2-TRPV4 clones did not show doublets (Fig. 2D,4A). Instead, two clones (#1 and #3) showed a new band at the lower end, possibly a truncated form of TRPV4 generated by a proteolytic process (Fig. 4A). In all three KPT2-TRPV4 cells, TRPV4 expression was uniformly localized at the cell membrane, with some diffuse somatic labeling (Fig. 4C,D). TRPV4 channels can induce $Ca^{2+}$ influx in response to hypotonic stimulus or TRPV4-specific activator 4α-phorbol 12,13-didecanoate (4α-PDD) (Liedtke et al., 2000; Strotmann et al., 2000; Watanabe et al., 2002). To confirm that KPT2-TRPV4 cells express functional TRPV4, calcium transients in response to hypotonicity and 4α-PDD were examined by fura-2 ratiometry. KPT2-TRPV4 cells exhibited intracellular $Ca^{2+}$ increase in response to hypotonicity or 4α-PDD with different time courses, with peak $Ca^{2+}$ influx occurred at 50 seconds of exposure to hypotonicity while $Ca^{2+}$ influx was yet to reach peak after 160 seconds of 4α-PDD treatment (Fig. 4E). KPT2-pBabe cells did not respond to either

NIH-PA Author Manuscript

NIH-PA Author Manuscript

NIH-PA Author Manuscript

stimulus, confirming that the $Ca^{2+}$ influx observed in KPT2-TRPV4 is dependent on TRPV4 (Fig. 4E).

After a 30-second treatment with GTTR in the presence of extracellular $Ca^{2+}$, there was no significant difference in GTTR uptake among all KPT2-TRPV4 and KPT2-pBabe cells (Fig. 5A,B,E). In the absence of extracellular $Ca^{2+}$, all KPT2-TRPV4 cells took up significantly more GTTR than the three KPT2-pBabe cells (Fig. 5C,D,E). In the presence of extracellular $Ca^{2+}$, GTTR uptake levels observed in these KPT2-derived cell lines were slightly higher than parental KPT2 cells (data not shown). This may be due to gene expression alteration caused by puromycin in medium and/or retrovirus used for cell line generation. The fluorescence intensity of cytoplasmic GTTR was quantified for KPT2-pBabe and KPT2-TRPV4 cells in the presence and absence of extracellular $Ca^{2+}$ (Fig. 5E). While there was no significant difference in the mean GTTR levels in the presence of extracellular $Ca^{2+}$, there was a statistically significant increase (>1.6-fold, $p<0.01$) in KPT2-TRPV4 cells compared to KPT2-pBabe in the absence of extracellular $Ca^{2+}$.

Mammalian inner ear endolymph is low in $Ca^{2+}$ concentration (0.023 mM) (Lang et al., 2007), and low extracellular $Ca^{2+}$ favors aminoglycoside entry into hair cells in vitro (Marcotti et al., 2005). Low $Ca^{2+}$ at 0.05 mM instead of no $Ca^{2+}$ was sufficient to enhance GTTR uptake in KPT2-TRPV4 cells compared to KPT2-pBabe (Fig. 5E).

## GTTR uptake in KPT2-TRPV4 cells is dependent on TRPV4 channel

KPT2 cell clones that express M680D mutant of TRPV4 (KPT2-M680D) were generated to further determine the role of TRPV4 in GTTR uptake. M680D mutation abolishes $Ca^{2+}$ selectivity in TRPV4 channel by altering channel pore properties (Voets et al., 2002; Nilius et al., 2004). M680D mutant expression was localized at the cell membrane and expression levels in KPT2-M680D cells were similar to TRPV4 in KPT2-TRPV4 (Fig. 6A-C). After a 30-second GTTR treatment, GTTR uptake in KPT2-M680D cells was not enhanced by extracellular $Ca^{2+}$ removal, suggesting that enhanced GTTR uptake in KPT2-TRPV4 cells is likely by GTTR permeating the TRPV4 channel pore (Fig. 6D).

A non-specific TRP channel inhibitor Ruthenium Red (RR) was co-administered with GTTR to further test if TRPV4 contributes to GTTR uptake in KPT2-TRPV4 cells. After a 30-second GTTR treatment with 50 μM RR in the absence of extracellular $Ca^{2+}$, there were significantly lower levels of GTTR fluorescence in KPT2-pBabe and KPT2-TRPV4 cells compared to cells without RR treatment (Fig. S1 in Supplemental Materials). Although GTTR uptake inhibition by RR was greater in KPT2-TRPV4 cells, KPT2-pBabe cells also showed significant inhibition of GTTR uptake by RR (Fig. S1 in Supplemental Materials). It is possible that KPT2-pBabe expresses other non-selective cation channels that are involved in aminoglycoside uptake, and these channels are also inhibited by RR.

## GTTR clearance from KPT2-TRPV4 in an endolymph-like extracellular environment

Inner ear hair cells take up aminoglycosides from endolymph by endocytosis or ion channel permeation (Hashino et al., 1995; Marcotti et al., 2005). To determine if cells can clear aminoglycosides into an endolymph-like extracellular environment, clearance of GTTR from cells was measured by loss of GTTR fluorescence following incubation in endolymph-like buffer (low $Na^{+}$, high $K^{+}$, low $Ca^{2+}$). To ensure sufficient GTTR levels in KPT2-pBabe cells at the initial time point, all cells were treated with GTTR in PBS with 1.25 mM $Ca^{2+}$ for 1 minute, to enable comparative assessment of GTTR clearance. At the initial time point (Fig. 7A,D), there were similar GTTR levels in all KPT-pBabe and KPT2-TRPV4 cell lines. After incubation in endolymph-like buffer for 5 or 10 minutes at 37°C to facilitate temperature-dependent TRPV4 activity, both cell lines had much lower GTTR levels

NIH-PA Author Manuscript

NIH-PA Author Manuscript

NIH-PA Author Manuscript

compared to the initial time point (Fig. 7A-F). However, KPT2-TRPV4 cells showed significantly higher GTTR levels compared to KPT2-pBabe cells after 10 minutes (Fig. 7A-I), which was confirmed for all the three KPT2-pBabe and three KPT2-TRPV4 cell lines. It is likely that the inward current induced by TRPV4 in the endolymph-like environment prevents cells from releasing GTTR. GTTR clearance rate in KPT2-M680D cells was similar to KPT2-pBabe cells (data not shown), suggesting that GTTR retention in KPT2-TRPV4 cells is dependent on TRPV4 channel pore permeability. In KPT2-TRPV4 cells, GTTR levels appeared slightly higher after 10 minutes than 5 minutes of clearance (Fig. 7E,F,I), possibly because cells started to contract to smaller sizes in response to the low $Ca^{2+}$ environment and GTTR became more concentrated in the cells. In extracellular buffer similar to DMEM (high $Na^{+}$, low $K^{+}$, high $Ca^{2+}$), there was no significant difference in GTTR clearance between KPT2-pBabe and KPT2-TRPV4, confirming that the TRPV4-dependent GTTR retention requires an endolymph-like extracellular environment (data not shown). Since RR is known to block the inward current induced by TRPV4, but not the outward current (Voets et al., 2002), cells were treated with RR during GTTR clearance to block the inward current. In the presence of 10 μM RR in endolymph-like buffer, GTTR clearance was significantly accelerated in KPT2-TRPV4 (Fig. 7G,H). These results suggest that, in an endolymph-like extracellular environment, aminoglycoside clearance is attenuated from cells that express TRPV4.

## Discussion

Further insight into aminoglycoside uptake mechanisms is essential to better understand the selective cytotoxicity of these drugs in the inner ear and kidney, which remains a major clinical issue. Aminoglycoside uptake occurs by endocytosis in kidney and sensory hair cells (Sandoval et al., 2000; Hashino et al., 1997). However, aminoglycosides also enhance reactive oxygen species generation within seconds of drug exposure in euthermic cells at room temperature (Hirose et al., 1997), which is too fast to be accounted for endocytosis (Mamdouh et al., 1996). We have previously reported evidence that aminoglycoside uptake also occurs by nonendocytotic mechanisms, and more specifically, by cation channel permeation (Myrdal et al., 2005; Myrdal and Steyger, 2005).

Gentamicin-Texas Red (GTTR) conjugate has proven to be useful in studying the endocytosis of aminoglycosides and subsequent intracellular trafficking (Sandoval et al., 2000; Sandoval and Molitoris, 2004). Although the relative molecular mass of GTTR is larger than that of untagged gentamicin, this does not affect its ability to permeate directly into the cytoplasm, and this distribution has been verified using gentamicin immunocytochemistry (Myrdal et al., 2005). Using GTTR, we have previously shown that aminoglycoside uptake in kidney cells can be regulated by cellular potential, pH, extracellular cations ($Ca^{2+}$, $Gd^{3+}$, $La^{3+}$), and non-specific cation channel blocker Ruthenium Red (RR) (Myrdal et al., 2005; Myrdal and Steyger, 2005). Importantly, TRPV1 activators resiniferatoxin and anandamide enhance aminoglycoside uptake in Madin-Darby canine kidney (MDCK) cells (Myrdal et al., 2005). However, TRPV1 expression is relatively low in the kidney and stria vascularis (Sanchez et al., 2001; Wang et al., 2004; Takumida et al., 2005), although there is substantial expression in hair cells (Zheng et al., 2003; Takumida et al., 2005). In contrast, TRPV4 is a TRP channel that is highly expressed in the kidney, stria vascularis, and hair cells (Liedtke et al., 2000; Strotmann et al., 2000; Wissenbach et al., 2000; Delany et al., 2001; Takumida et al., 2005; Shen et al., 2006). It has been suggested that TRPV4 responds to changes in interstitial osmolarity (e.g. urine flow rate change), and transmits the tonicity signals to more distal tubule segments where “fine-tuning” regulation of salt and water balance takes place (Cohen, 2005). In the inner ear, TRPV4 expression in the stria vascularis has been thought to play a role in maintaining the ionic composition of endolymph and the endocochlear potential (Liedtke et al., 2000). It has been hypothesized

NIH-PA Author Manuscript

NIH-PA Author Manuscript

NIH-PA Author Manuscript

that aminoglycosides take a trans-strial pathway to cross the stria vascularis and enter endolymph (Dai and Steyger, 2008). Therefore, we sought to determine if TRPV4 is involved in cochlear trafficking of aminoglycosides.

Virtually all cells take up aminoglycosides, and most clear the drugs (Dai et al., 2006). However, the kidney and inner ear retain aminoglycosides and are susceptible to aminoglycoside-induced toxicity, and share other common characteristics, such as fluid and ion regulation, and protein expression of various ion channels and transporters (Lang et al., 2007). Therefore, we used kidney cells as an in vitro model to study aminoglycoside uptake and clearance. Existing kidney proximal and distal tubule cell lines such as Opossum Kidney (OK) and MDCK cells are from different species, genetic backgrounds, and were generated by different methods. For this reason, we developed new kidney cell lines from mice with similar genetic backgrounds by spontaneous immortalization. In support of our cell line generation method, immortalized kidney proximal and distal tubule cell lines tend to retain differentiated cell-specific functions (Vandewalle, 2002).

### Cellular GTTR uptake mechanisms

GTTR uptake was greater in KPT2 cells than in KDT3 cells in the presence of extracellular $Ca^{2+}$. Removal of extracellular $Ca^{2+}$ increased GTTR uptake levels in KPT2 and KDT3 cells, with significantly greater enhancement in KDT3. Since removing extracellular $Ca^{2+}$ increases inward currents mediated by TRPV4 (Voets et al., 2002), TRPV4 may largely be responsible for the enhanced GTTR uptake in KDT3 cells. In KDT3 cells, TRPV4 is highly expressed in the basolateral membrane, but there is also some expression in the apical membrane (Fig. 2G). This suggests that apical TRPV4 channels may participate in GTTR uptake mechanisms in the absence of extracellular $Ca^{2+}$. In physiological extracellular $Ca^{2+}$, tight junctions near the lumenal surface of KDT3 cells may restrict GTTR access to TRPV4 in the basolateral membrane. It is possible that extracellular $Ca^{2+}$ removal opened tight junctions (Pitelka et al., 1983), providing GTTR access to the basolateral membrane of KDT3 cells to allow greater uptake via TRPV4 channels.

KPT2 cells take up more GTTR than KDT3 cells in the presence of extracellular $Ca^{2+}$, and show modest enhancement of GTTR uptake by removing extracellular $Ca^{2+}$. Since KPT2 cells lack TRPV4 expression, it likely expresses other cation channels that are involved in GTTR uptake. TRPV1 and purinergic $P2X_2$ receptor may be such channels because these are permeable to a large cationic dye FM1-43 (Meyers et al., 2003), although we did not detect TRPV1 in KPT2 by immunoblot analysis (T. Karasawa and P. S. Steyger, unpublished). These channels may also mediate a moderate increase in inward currents upon removal of extracellular $Ca^{2+}$, and could therefore mediate GTTR uptake in KPT2 cells. Inhibition of GTTR uptake by RR in KPT2 cells also implicates other channels in GTTR uptake mechanisms. Similar GTTR uptake levels in KPT2 and KDT3 cells in the absence of extracellular $Ca^{2+}$ suggests that there were sufficient uptake routes at the cell membrane for GTTR that virtually no barrier existed to block GTTR entry.

To determine if TRPV4 plays a role in aminoglycoside uptake in TRPV4-expressing cells, we generated KPT2-derived cell lines that express TRPV4 (KPT2-TRPV4) and that do not (KPT2-pBabe), and compared GTTR uptake levels between these cell lines. Although KPT2-TRPV4 cells take up more GTTR by extracellular $Ca^{2+}$ removal, and can respond to TRPV4 activator 4α-PDD in the fura-2 ratiometry assay, we did not observe GTTR uptake enhancement by 4α-PDD in KPT2-TRPV4 cells (data not shown). In the presence of extracellular $Ca^{2+}$, 4α-PDD induces an inward current that is rapidly inactivated by intracellular $Ca^{2+}$ (Nilius et al., 2004). It is possible that the inward current duration induced by 4α-PDD is not sufficient for enhancing GTTR uptake in the presence of extracellular $Ca^{2+}$. It is also possible that the effect induced by 4α-PDD is too slow to appear during the

NIH-PA Author Manuscript

NIH-PA Author Manuscript

NIH-PA Author Manuscript

GTTR treatment. In the absence of extracellular $Ca^{2+}$, the inward current induced by 4α-PDD lasts for several minutes (Nilius et al, 2004). However, removal of extracellular $Ca^{2+}$ itself induces a large inward current (Voets et al., 2002), which is likely the reason that additive effects by 4α-PDD and extracellular $Ca^{2+}$ removal could not be observed for GTTR uptake.

M680 residue of TRPV4 is located within the $K^+$ channel signature sequence, which is the crucial pore region of $K^+$ channels (Doyle et al., 1998; Zhou et al., 2001). The M680D mutation abolishes the $Ca^{2+}$ selectivity of the TRPV4 pore (Voets et al., 2002). We found that extracellular $Ca^{2+}$ removal does not significantly enhance GTTR uptake in KPT2-derived cell lines expressing the M680D mutant (KPT2-M680D). This strongly indicates that GTTR uptake by KPT2-TRPV4 cells is permeation through the TRPV4 channel, since the mutation appears to affect the channel pore properties only, and the mutant in KPT2-M680D cells is expressed at similar levels and localization compared to the wild-type in KPT2-TRPV4 cells.

## Cochlear mechanisms of aminoglycoside uptake

In vivo, aminoglycosides likely enter hair cells from endolymph via both endocytosis and mechanoelectrical transduction channels (Hashino et al., 1995; Hiel et al., 1992; Marcotti et al., 2005). The machanoelectrical transduction channel is permeable to dihydrostreptomycin and this permeation is attenuated by 1.3 mM extracellular $Ca^{2+}$, and enhanced at low extracellular $Ca^{2+}$ (Marcotti et al., 2005). Although it is yet to be determined whether or not TRPV4 is a part of the mechanoelectrical channel, hair cells express TRPV4 in their apical membranes and stereocilia (Fig. 1) (Liedtke et al., 2000; Takumida et al., 2005; Shen et al., 2006). It is interesting to speculate that TRPV4 in the apical membrane of hair cells, including stereocilia, facilitates rapid aminoglycoside uptake into the cells due to the ultra-low $Ca^{2+}$ environment in endolymph (Lang et al., 2007).

In this study, we also showed that aminoglycoside clearance is attenuated from cells that express TRPV4 in an endolymph-like extracellular environment. The large inward current induced by TRPV4 may prevent cell from releasing aminoglycosides. KPT2-M680D cells did not show TRPV4-dependent GTTR retention, supporting that TRPV4 channel activity is responsible for aminoglycoside retention. It is possible that TRPV4 or other TRP channels expressed in the apical membrane contribute to aminoglycoside retention in hair cells. TRPV4 does not likely play a role in aminoglycoside retention in most other cells, including kidney distal tubule cells, because there was no TRPV4-dependent GTTR retention in cells with buffer of typical extracellular ion components (DMEM).

Although the stria vascularis of the inner ear is not thought to be as susceptible as hair cells, aminoglycosides can also damage the stria vascularis (Forge and Fradis, 1985; Kusunoki et al., 2004), which in turn leads to auditory dysfunction. In the stria vascularis, we identified high levels of TRPV4 expression in the lumenal membrane of marginal cells, bathed in endolymph (Fig. 1). Therefore, it is possible that TRPV4 contribute to aminoglycoside retention in the stria vascularis by preventing drug clearance from endolymph.

A better understanding of the aminoglycoside permeation through TRPV4 and other non-selective cation channels will further our knowledge of how systemic aminoglycosides enter the cochlear fluids and hair cells. This will enable the development of new strategies to block aminoglycoside entry in there, and prevent aminoglycoside-induced hearing loss and vestibular disorders following systemic administration.

NIH-PA Author Manuscript

NIH-PA Author Manuscript

NIH-PA Author Manuscript

## Materials and Methods

### Cell culture

Mouse kidney cell lines were generated as described previously (Turker et al., 1999). Briefly, mouse kidney was minced using a surgical blade, and digested with 0.07 mg/ml Liberase Blenzyme (Roche Diagnostics Corp.) at 37°C for 45 minutes, and spun down. Cells were resuspended in DMEM supplemented with 15% FBS, and plated in 100-mm plates to obtain primary cultures. Primary cultures were maintained in DMEM with 15% FBS, and several clones were expanded to identify cells that had undergone spontaneous immortalization. Two kidney proximal and a distal tubule cell lines were identified based on morphology and TRPV4 expression, and designated as KPT1, KPT2, and KDT3, respectively. These cell lines were maintained in DMEM with 10% FBS. KPT2-derived cell lines generated by retroviral transduction were maintained in 2.5 μg/ml puromycin-containing DMEM with 10% FBS. Madin-Darby canine kidney cells (MDCK) were maintained in MEM-α with 10% FBS.

### RT-PCR

Total RNA from cells was isolated by using RNeasy Mini kit (Qiagen), and first-strand cDNA was synthesized from 1 μg of total RNA in a 20 μl reaction mixture containing oligo(dT) to hybridize to 3' poly(A) tails of mRNA, and SuperScript II Reverse Transcriptase (Invitrogen) to catalyze synthesis. RNA template was removed after cDNA synthesis by digestion with RNase H. For PCR, 2 μl of the reverse-transcribed cDNA was used in each reaction catalyzed by AmpliTaq DNA polymerase (Applied Biosystems). The PCR condition used is the initial 95°C for 2 minutes followed by 35 cycles of 95°C for 30 seconds, 60°C for 30 seconds, and 72°C for 1 minute for all reactions. Primers used are: 5'-CCTTCGTGCTCCTGTTGAAC-3' and 5'-CACCACTTCATCTGCGCTTG-3' for mouse TRPV4 (410 bp fragment), 5'-TGTTGCTCTAGACTTCGAGCAG-3' and 5'-ACCGATCCACACAGAGTACTTG-3' for mouse β-actin (373 bp fragment). PCR was performed in an Applied Biosystems thermal cycler. PCR products were analyzed by electrophoresis in 2% agarose gel.

### Immunoblotting

Total proteins were extracted with lysis buffer (50 mM Tris at pH 7.5, 150 mM NaCl, 5 mM EDTA, 1% Triton X-100, 0.5% sodium deoxycholate) that contains the protease inhibitor cocktail (Sigma). The extracts were centrifuged at 13,000 rpm to remove cell debris, mixed with SDS sample buffer, and separated in 8% gel by SDS-polyacrylamide gel electrophoresis. The proteins were transferred to PVDF membranes (Millipore). The membrane was blocked with 5% non-fat dry milk in Tris-buffered saline containing 0.1% Tween 20 (TBST) for 1 hour and then incubated with TRPV4 antibody (a generous gift from Dr. Stefan Heller) at 1:5000 dilution, or actin antibody (Sigma) at 1:500 dilution overnight at 4°C. The blots were washed three times with TBST, incubated with horseradish peroxidase-conjugated secondary antibody for 1 hour at room temperature and washed again three times. The protein bands were detected by chemiluminescence using SuperSignal West Dura Extended Duration Substrate (Pierce).

### Immunofluorescence

To generate wholemounts and sections of the murine cochlea and kidney for immunolabeling, mice were fixed by transcardiac perfusion of 4% paraformaldehyde in PBS, excised and immersion fixed overnight with 4% paraformaldehyde plus 0.5% Triton X-100 (FATX). The cochlea was dissected and lateral wall exposed, and bone was removed from the stria vascularis. The kidney was vibratome-sectioned at 100 μm thickness. Tissues

NIH-PA Author Manuscript

NIH-PA Author Manuscript

NIH-PA Author Manuscript

and sections were blocked with PBS containing 10% normal goat serum and 1% BSA, incubated with rabbit TRPV4 antibody at 1:2000 dilution for 1 hour, and then with Alexa-488-conjugated goat anti-rabbit antibody for 1 hour, prior to washing, labeling with Alexa-568 phalloidin at 1:100 for 1 hour. Specimens were then washed, post-fixed with 4% paraformaldehyde, rinsed and mounted using VectaShield and imaged using confocal microscopy (Steyger et al., 2003).

### Retroviral tranduction

Rat TRPV4 cDNA (a generous gift from Dr. Wolfgang Liedtke) in pcDNA3.1 was amplified by PCR, using PfuUltra DNA polymerase (Stratagene) and the primers 5'-TTTGGATCCACCATGGCAGATCCTGGTGATG-3' and 5'-TTTGTCGACTACAGTGGTGCGTCCTCCGC-3'. The PCR product was digested with BamHI and SalI, and subcloned into a retroviral expression plasmid pBabe-puro. For M680D mutant of TRPV4, QuikChange Site-Directed Mutagenesis Kit (Stratagene) with primers 5'-CAAGCTCACCATCGGCGACGGCGACCTGGAGATGC-3' and 5'-GCATCTCCAGGTCGCCGTCGCCGATGGTGAGCTTG-3' were used to generate the point mutation. The resultant plasmids were sequenced to confirm that there is no false mutation within the coding region of TRPV4. Each retroviral expression construct or pBabe-puro was transfected into Phoenix Eco packaging cells using LipofectAMINE 2000 (Invitrogen). After 72 hours, the retrovirus-containing supernatant was collected, and diluted (1:1000) with growth medium and added to KPT2 cell cultures. This medium was removed after 24 hours, and growth medium supplemented with puromycin (2.5 μg/ml) was added to select for retrovirus-infected cells. From dozens of surviving cells after several days of puromycin treatment, several clones were selected and expanded.

### Intracellular calcium measurement by fura-2 ratiometry

Cells were trypsinized, washed, and resuspended in 10 ml of HBSS (130 mM NaCl, 4.7 mM KCl, 1.25 mM $CaCl_2$, 1.18 mM $MgSO_4$, 5 mM glucose, 15 mM HEPES, pH 7.5) supplemented with 2 μM fura-2-AM and 100 μl of 2% Pluronic F-127 (20% stock solution in DMSO, Molecular Probes, Inc.) per 100 mm dish, and then incubated for 45 minutes at 37°C. Cells were pelleted at 1,000 × *g* for 5 minutes at 25°C, resuspended with 1-2 ml of HBSS to achieve final concentration of ~2-8 × $10^7$ cells/ml, and maintained on ice for 30 minutes. The suspended fura-2-loaded cells (50 μl) were assayed for intracellular $Ca^{2+}$ concentration in a cuvette filled with pre-warmed (37°C) HBSS under constant gentle stirring (2-ml final volume) as previously reported (Xu et al., 2003). Fluorescent emission was monitored at 510 nm and recorded once per second in the presence of alternating excitation at 340 nm and 380 nm using a Hitachi F-2500 fluorescence spectrophotometer (Hitachi Instruments, Inc.). For treatment with TRPV4 agonist 4α-phorbol 12,13-didecanoate (4α-PDD), the agonist was added directly to the cuvette in a small volume at final concentration of 50 nM, after a stable baseline fluorescence ratio had been achieved (not shown in figure). For treatment with hypotonicity, cells were added directly to hypotonic HBSS (150 mOsmol/kg$H_2O$). Calibration of the fura-2 signal was performed as previously described (Roullet et al., 1997) using fura-2·$Ca^{2+}$ dissociation constant of 224 nM (Grynkiewicz et al., 1985).

### Gentamicin-Texas Red (GTTR) uptake and clearance, and confocal microscopy

GTTR was generated as described previously (Myrdal et al., 2005). Cells plated on 8-well chambered coverslips were washed with PBS with or without 1.25 mM $CaCl_2$ twice, incubated with 5 μg/ml GTTR in PBS with or without 1.25 mM $CaCl_2$ for 30 seconds at room temperature, to preclude endocytosis. Cells were washed again with PBS three times to remove GTTR from extracellular buffer, and fixed with FATX for 45 minutes. For Ruthenium Red (RR) treatment, RR was added to GTTR solution at the final concentration

NIH-PA Author Manuscript

NIH-PA Author Manuscript

NIH-PA Author Manuscript

of 50 μM before cells were treated with GTTR. For GTTR clearance, cells were treated with GTTR for 1 minute under the same conditions as for GTTR uptake. After washing with PBS three times, cells were incubated in the clearance buffer (1.3 mM NaCl, 130 mM KCl, 30 mM $KHCO_3$, 0.05 mM $CaCl_2$, pH 7.5) with or without 10 μM RR for 5 or 10 minutes at 37°C prior to fixation with FATX. Buffer similar to DMEM was also tested for GTTR clearance, with components of 110 mM NaCl, 5.3 mM KCl, 44 mM $NaHCO_3$, 1.8 mM $CaCl_2$, 0.9 mM $NaH_2PO_4$, adjusted to pH 7.5. The distribution of GTTR fluorescence was examined using an 8-bit Bio-Rad 1024 ES scanning laser system. For each individual set of images to be compared, the same confocal settings were used, and two images per well were collected. There were two wells per experimental condition, and each experiment was performed at least three times, to confirm that the results were consistent. GTTR fluorescent intensity values were obtained by histogram function of the ImageJ software after removal of nuclei and intercellular pixels using Adobe Photoshop. Fluorescence intensity was compared only within each set of images or experiment, and was not compared between different experiments because different image acquisition settings were used for different experiments to obtain the best dynamic range.

## Supplementary Material

Refer to Web version on PubMed Central for supplementary material.

## Acknowledgments

We thank S. Heller for anti-TRPV4 antibody and W. Liedtke for TRPV4 cDNA and TRPV4-knockout mice. This work was supported by NIH NIDCD grants DC04555 (P.S.S.), P30 DC05983, T32 DC005945 and F32 DC008465 (T.K.), and by the Oregon Medical Research Foundation.

## References

Chen P, Segil N. p27(Kip1) links cell proliferation to morphogenesis in the developing organ of Corti. Development 1999;126:1581–1590. [PubMed: 10079221]

Cohen DM. TRPV4 and the mammalian kidney. Pflugers Arch 2005;451:168–175. [PubMed: 15988590]

Dai CF, Mangiardi D, Cotanche DA, Steyger PS. Uptake of fluorescent gentamicin by vertebrate sensory cells in vivo. Hear. Res 2006;213:64–78. [PubMed: 16466873]

Dai CF, Steyger PS. A systemic gentamicin pathway across the stria vascularis. Hear. Res 2008;235:114–124. [PubMed: 18082985]

Davies J, Davis BD. Misreading of ribonucleic acid code words induced by aminoglycoside antibiotics. The effect of drug concentration. J. Biol. Chem 1968;243:3312–3316. [PubMed: 5656371]

Delany NS, Hurle M, Facer P, Alnadaf T, Plumpton C, Kinghorn I, See CG, Costigan M, Anand P, Woolf CJ, et al. Identification and characterization of a novel human vanilloid receptor-like protein, VRL-2. Physiol. Genomics 2001;4:165–174. [PubMed: 11160995]

Doyle DA, Morais Cabral J, Pfuetzner RA, Kuo A, Gulbis JM, Cohen SL, Chait BT, MacKinnon R. The structure of the potassium channel: molecular basis of K+ conduction and selectivity. Science 1998;280:69–77. [PubMed: 9525859]

Forge A, Fradis M. Structural abnormalities in the stria vascularis following chronic gentamicin treatment. Hear. Res 1985;20:233–244. [PubMed: 4086385]

Forge A, Schacht J. Aminoglycoside antibiotics. Audiol. Neurootol 2000;5:3–22. [PubMed: 10686428]

Grohskopf LA, Huskins WC, Sinkowitz-Cochran RL, Levine GL, Goldmann DA, Jarvis WR. Use of antimicrobial agents in United States neonatal and pediatric intensive care patients. Pediatr. Infect. Dis. J 2005;24:766–773. [PubMed: 16148841]

NIH-PA Author Manuscript

NIH-PA Author Manuscript

NIH-PA Author Manuscript

Grynkiewicz G, Poenie M, Tsien RY. A new generation of $Ca^{2+}$ indicators with greatly improved fluorescence properties. J. Biol. Chem 1985;260:3440–3450. [PubMed: 3838314]

Hashino E, Shero M. Endocytosis of aminoglycoside antibiotics in sensory hair cells. Brain Res 1995;704:135–140. [PubMed: 8750975]

Hashino E, Shero M, Salvi RJ. Lysosomal targeting and accumulation of aminoglycoside antibiotics in sensory hair cells. Brain Res 1997;777:75–85. [PubMed: 9449415]

Hiel H, Schamel A, Erre JP, Hayashida T, Dulon D, Aran JM. Cellular and subcellular localization of tritiated gentamicin in the guinea pig cochlea following combined treatment with ethacrynic acid. Hear. Res 1992;57:157–165. [PubMed: 1733909]

Hirose K, Hockenbery DM, Rubel EW. Reactive oxygen species in chick hair cells after gentamicin exposure in vitro. Hear. Res 1997;104:1–14. [PubMed: 9119753]

Klein JO. Recent advances in management of bacterial meningitis in neonates. Infection 1984;12(Suppl 1):S44–51. [PubMed: 6397449]

Kusunoki T, Cureoglu S, Schachern PA, Sampaio A, Fukushima H, Oktay MF, Paparella MM. Effects of aminoglycoside administration on cochlear elements in human temporal bones. Auris Nasus Larynx 2004;31:383–388. [PubMed: 15571911]

Lang F, Vallon V, Knipper M, Wangemann P. Functional significance of channels and transporters expressed in the inner ear and kidney. Am. J. Physiol. Cell Physiol 2007;293:C1187–1208. [PubMed: 17670895]

Lee JE, Nakagawa T, Kim TS, Iguchi F, Endo T, Kita T, Murai N, Naito Y, Lee SH, Ito J. Signaling pathway for apoptosis of vestibular hair cells of mice due to aminoglycosides. Acta Otolaryngol. Suppl 2004;551:69–74. [PubMed: 15078083]

Liedtke W, Choe Y, Marti-Renom MA, Bell AM, Denis CS, Sali A, Hudspeth AJ, Friedman JM, Heller S. Vanilloid receptor-related osmotically activated channel (VR-OAC), a candidate vertebrate osmoreceptor. Cell 2000;103:525–535. [PubMed: 11081638]

Lowenheim H, Furness DN, Kil J, Zinn C, Gultig K, Fero ML, Frost D, Gummer AW, Roberts JM, Rubel EW, et al. Gene disruption of p27(Kip1) allows cell proliferation in the postnatal and adult organ of corti. Proc. Natl. Acad. Sci. USA 1999;96:4084–4088. [PubMed: 10097167]

Mamdouh Z, Giocondi MC, Laprade R, LeGrimellec C. Temperature dependence of endocytosis in renal epithelial cells in culture. Biochim. Biophys. Acta 1996;1282:171–173. [PubMed: 8703969]

Marcotti W, van Netten SM, Kros CJ. The aminoglycoside antibiotic dihydrostreptomycin rapidly enters mouse outer hair cells through the mechano-electrical transducer channels. J. Physiol 2005;567:505–521. [PubMed: 15994187]

Meyers JR, MacDonald RB, Duggan A, Lenzi D, Standaert DG, Corwin JT, Corey DP. Lighting up the senses: FM1-43 loading of sensory cells through nonselective ion channels. J. Neurosci 2003;23:4054–4065. [PubMed: 12764092]

Mingeot-Leclercq MP, Tulkens PM. Aminoglycosides: nephrotoxicity. Antimicrob. Agents Chemother 1999;43:1003–1012. [PubMed: 10223907]

Myrdal SE, Johnson KC, Steyger PS. Cytoplasmic and intra-nuclear binding of gentamicin does not require endocytosis. Hear. Res 2005;204:156–169. [PubMed: 15925201]

Myrdal SE, Steyger PS. TRPV1 regulators mediate gentamicin penetration of cultured kidney cells. Hear. Res 2005;204:170–182. [PubMed: 15925202]

Nilius B, Vriens J, Prenen J, Droogmans G, Voets T. TRPV4 calcium entry channel: a paradigm for gating diversity. Am. J. Physiol. Cell Physiol 2004;286:C195–205. [PubMed: 14707014]

Noller HF. Ribosomal RNA and translation. Annu. Rev. Biochem 1991;60:191–227. [PubMed: 1883196]

Pirvola U, Xing-Qun L, Virkkala J, Saarma M, Murakata C, Camoratto AM, Walton KM, Ylikoski J. Rescue of hearing, auditory hair cells, and neurons by CEP-1347/KT7515, an inhibitor of c-Jun N-terminal kinase activation. J. Neurosci 2000;20:43–50. [PubMed: 10627579]

Pitelka DR, Taggart BN, Hamamoto ST. Effects of extracellular calcium depletion on membrane topography and occluding junctions of mammary epithelial cells in culture. J. Cell Biol 1983;96:613–624. [PubMed: 6403552]

NIH-PA Author Manuscript

NIH-PA Author Manuscript

NIH-PA Author Manuscript

Roullet JB, Luft UC, Xue H, Chapman J, Bychkov R, Roullet CM, Luft FC, Haller H, McCarron DA. Farnesol inhibits L-type $Ca^{2+}$ channels in vascular smooth muscle cells. J. Biol. Chem 1997;272:32240–32246. [PubMed: 9405427]

Sanchez JF, Krause JE, Cortright DN. The distribution and regulation of vanilloid receptor VR1 and VR1 5' splice variant RNA expression in rat. Neuroscience 2001;107:373–381. [PubMed: 11718993]

Sandoval RM, Dunn KW, Molitoris BA. Gentamicin traffics rapidly and directly to the Golgi complex in LLC-PK(1) cells. Am. J. Physiol. Renal Physiol 2000;279:F884–890. [PubMed: 11053049]

Sandoval RM, Molitoris BA. Gentamicin traffics retrograde through the secretory pathway and is released in the cytosol via the endoplasmic reticulum. Am. J. Physiol. Renal Physiol 2004;286:F617–624. [PubMed: 14625200]

Shen J, Harada N, Kubo N, Liu B, Mizuno A, Suzuki M, Yamashita T. Functional expression of transient receptor potential vanilloid 4 in the mouse cochlea. Neuroreport 2006;17:135–139. [PubMed: 16407759]

Steyger PS, Peters SL, Rehling J, Hordichok A, Dai CF. Uptake of gentamicin by bullfrog saccular hair cells in vitro. J. Assoc. Res. Otolaryngol 2003;4:565–578. [PubMed: 14605921]

Strotmann R, Harteneck C, Nunnenmacher K, Schultz G, Plant TD. OTRPC4, a nonselective cation channel that confers sensitivity to extracellular osmolarity. Nat. Cell Biol 2000;2:695–702. [PubMed: 11025659]

Taber HW, Mueller JP, Miller PF, Arrow AS. Bacterial uptake of aminoglycoside antibiotics. Microbiol. Rev 1987;51:439–457. [PubMed: 3325794]

Takeuchi S, Ando M, Sato T, Kakigi A. Three-dimensional and ultrastructural relationships between intermediate cells and capillaries in the gerbil stria vascularis. Hear. Res 2001;155:103–112. [PubMed: 11335080]

Takumida M, Kubo N, Ohtani M, Suzuka Y, Anniko M. Transient receptor potential channels in the inner ear: presence of transient receptor potential channel subfamily 1 and 4 in the guinea pig inner ear. Acta Otolaryngol 2005;125:929–934. [PubMed: 16193584]

Tian W, Salanova M, Xu H, Lindsley JN, Oyama TT, Anderson S, Bachmann S, Cohen DM. Renal expression of osmotically responsive cation channel TRPV4 is restricted to water-impermeant nephron segments. Am. J. Physiol. Renal Physiol 2004;287:F17–24. [PubMed: 15026302]

Turker MS, Gage BM, Rose JA, Elroy D, Ponomareva ON, Stambrook PJ, Tischfield JA. A novel signature mutation for oxidative damage resembles a mutational pattern found commonly in human cancers. Cancer Res 1999;59:1837–1839. [PubMed: 10213488]

Vandewalle A. Immortalized renal proximal and collecting duct cell lines derived from transgenic mice harboring L-type pyruvate kinase promoters as tools for pharmacological and toxicological studies. Cell Biol. Toxicol 2002;18:321–328. [PubMed: 12240963]

Voets T, Prenen J, Vriens J, Watanabe H, Janssens A, Wissenbach U, Bodding M, Droogmans G, Nilius B. Molecular determinants of permeation through the cation channel TRPV4. J. Biol. Chem 2002;277:33704–33710. [PubMed: 12093812]

Wang C, Hu HZ, Colton CK, Wood JD, Zhu MX. An alternative splicing product of the murine trpv1 gene dominant negatively modulates the activity of TRPV1 channels. J. Biol. Chem 2004;279:37423–37430. [PubMed: 15234965]

Watanabe H, Davis JB, Smart D, Jerman JC, Smith GD, Hayes P, Vriens J, Cairns W, Wissenbach U, Prenen J, et al. Activation of TRPV4 channels (hVRL-2/mTRP12) by phorbol derivatives. J. Biol. Chem 2002;277:13569–13577. [PubMed: 11827975]

Wissenbach U, Bodding M, Freichel M, Flockerzi V. Trp12, a novel Trp related protein from kidney. FEBS Lett 2000;485:127–134. [PubMed: 11094154]

Xu H, Zhao H, Tian W, Yoshida K, Roullet JB, Cohen DM. Regulation of a transient receptor potential (TRP) channel by tyrosine phosphorylation. SRC family kinase-dependent tyrosine phosphorylation of TRPV4 on TYR-253 mediates its response to hypotonic stress. J. Biol. Chem 2003;278:11520–11527. [PubMed: 12538589]

Zheng J, Dai C, Steyger PS, Kim Y, Vass Z, Ren T, Nuttall AL. Vanilloid receptors in hearing: altered cochlear sensitivity by vanilloids and expression of TRPV1 in the organ of corti. J. Neurophysiol 2003;90:444–455. [PubMed: 12660354]

NIH-PA Author Manuscript

NIH-PA Author Manuscript

NIH-PA Author Manuscript

Zhou Y, Morais-Cabral JH, Kaufman A, MacKinnon R. Chemistry of ion coordination and hydration revealed by a $K^+$ channel-Fab complex at 2.0 Å resolution. Nature 2001;414:43–48. [PubMed: 11689936]

NIH-PA Author Manuscript
NIH-PA Author Manuscript
NIH-PA Author Manuscript



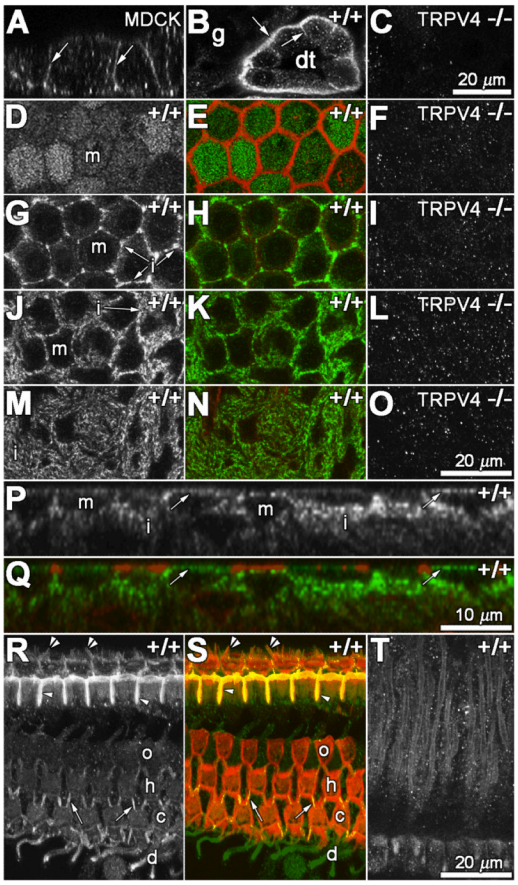


**Fig. 1.**

TRPV4 expression in kidney and inner ear. In MDCK cells, TRPV4 immunofluorescence was preferentially localized at the basolateral membrane (arrows in A). TRPV4 was also localized at the basolateral membranes (arrows) of wild-type (+/+) murine kidney distal tubule cells, but not in adjacent glomerular regions (g, in B), nor in the kidney of TRPV4-deficient mice (-/-, in C). In wholemounts of the stria vascularis from wild-type mice, TRPV4 was localized at the lumenal surface of marginal cells (m in D; green in E) at the level of the actiniferous tight junctions (red) between adjacent marginal cells (E, same focal plane as D). There was negligible TRPV4 immunoexpression at the lumenal surface of marginal cells of TRPV4-deficient mice (F). In a focal series of the cells shown in D and E, below the actiniferous tight junctions, only weak TRPV4 immunofluorescence occurred in the somata of marginal cells, but was prominent at the periphery of marginal cells (i in G, green in H). There was no TRPV4 expression detected in the somata of marginal cells from TRPV4-deficient mice (I). At lower focal planes than in G and H, strong, characteristic TRPV4 expression (J,M, green in K,N) was localized in intermediate (i) cells. TRPV4 expression could not be detected in the intra-strial tissues of TRPV4-deficient mice (L,O). In z-sections of the stria vascularis, TRPV4 immunolabeling was clearly associated with the lumenal surface (arrows) of the marginal cells (m), between the actiniferous tight junctions, and in the intermediate cells (i) below the weakly-labeled somata of marginal cells of wild-type mice (P,Q). In the organ of Corti, TRPV4 expression was most prominent in the region of tight junctions between adjacent pillar cells (arrowheads), and also between adjacent Deiters' cell phalangeal apices (arrows; R,S). The stereocilia of inner hair cells displayed TRPV4 expression (double arrowheads; R,S). TRPV4 expression was also present in Deiters' cell phalanges (d), but only weakly in OHCs (ohc) and spiral ganglion cells (T).

Scale bar of 20 μm in C also applies for A, B. Scale bar of 20 μm in O also applies for D-N, R-T. Scale bar of 10 μm in Q also applies for P.

NIH-PA Author Manuscript
NIH-PA Author Manuscript
NIH-PA Author Manuscript

NIH-PA Author Manuscript

NIH-PA Author Manuscript

NIH-PA Author Manuscript

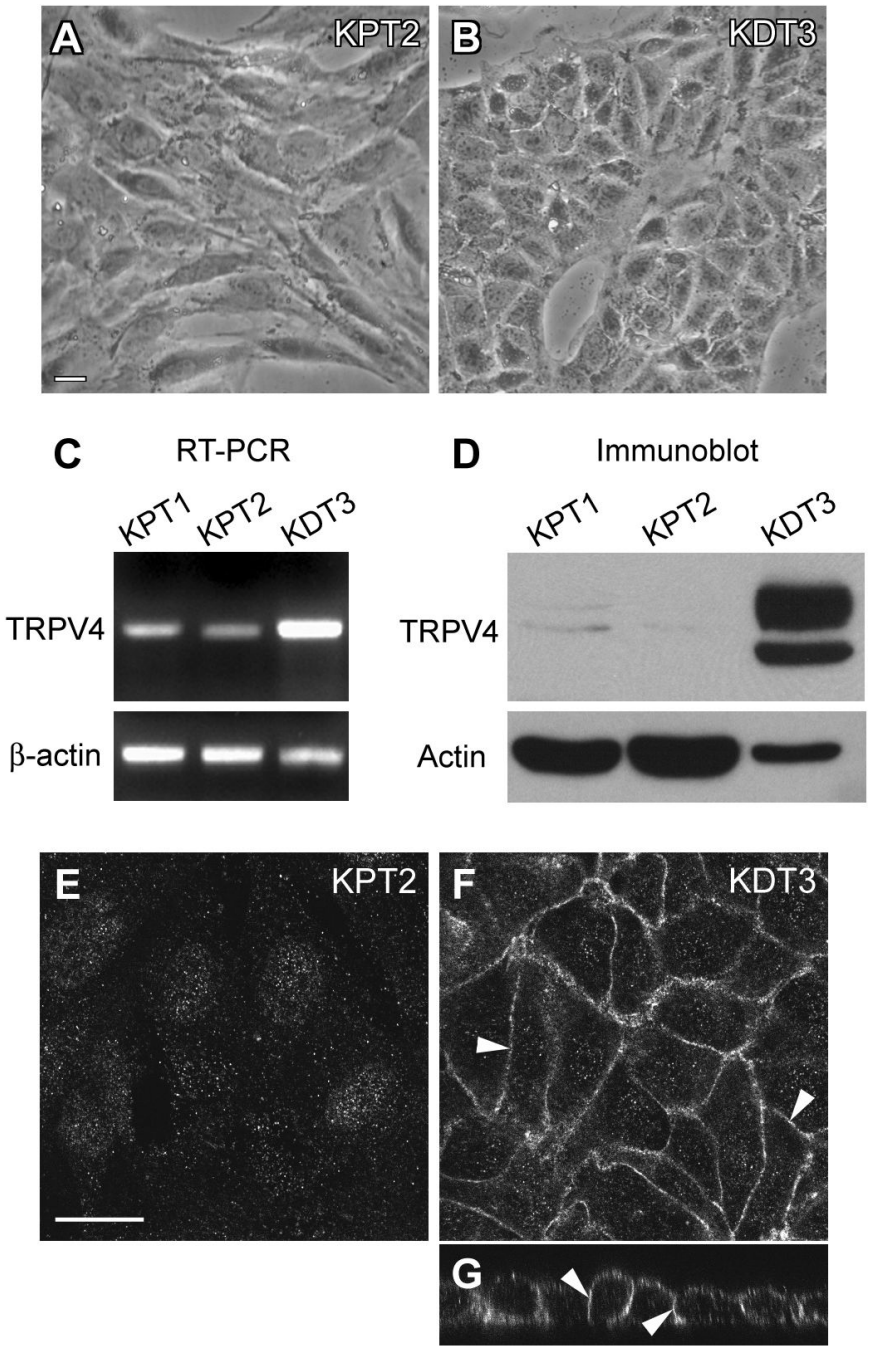


**Fig. 2.**

New kidney cell line generation and TRPV4 expression. By spontaneous immortalization, three cell lines were generated from primary murine kidney cultures. Bright-field images show KPT2 cells with a fibroblastic morphology (A), and KDT3 cells with an epithelial/cobblestone appearance and smooth edges to cell clusters (B). TRPV4 expression levels were determined by RT-PCR (C) and immunoblotting (D). KDT3 cells showed a high level of TRPV4 expression while KPT1 and KPT2 showed weak TRPV4 expression or possibly non-specific bands. Lower levels of β-actin in the RT-PCR (C) and actin in the immunoblot (D) suggest that KDT3 cells express β-actin and possibly other actin isoforms at lower levels compared to KPT1 and KPT2. TRPV4 expression was negligible in KPT2 cells (E).

NIH-PA Author Manuscript

NIH-PA Author Manuscript

NIH-PA Author Manuscript

Immunofluorescence showed TRPV4 localization at the basolateral membrane (arrowheads) of KDT3 cells (F). Orthogonal view of KDT3 cells shows TRPV4 expression in the basolateral membrane (arrowheads) (G). Bar in A applies for B (20 μm). Bar in E applies for F and G (20 μm).

NIH-PA Author Manuscript
NIH-PA Author Manuscript
NIH-PA Author Manuscript



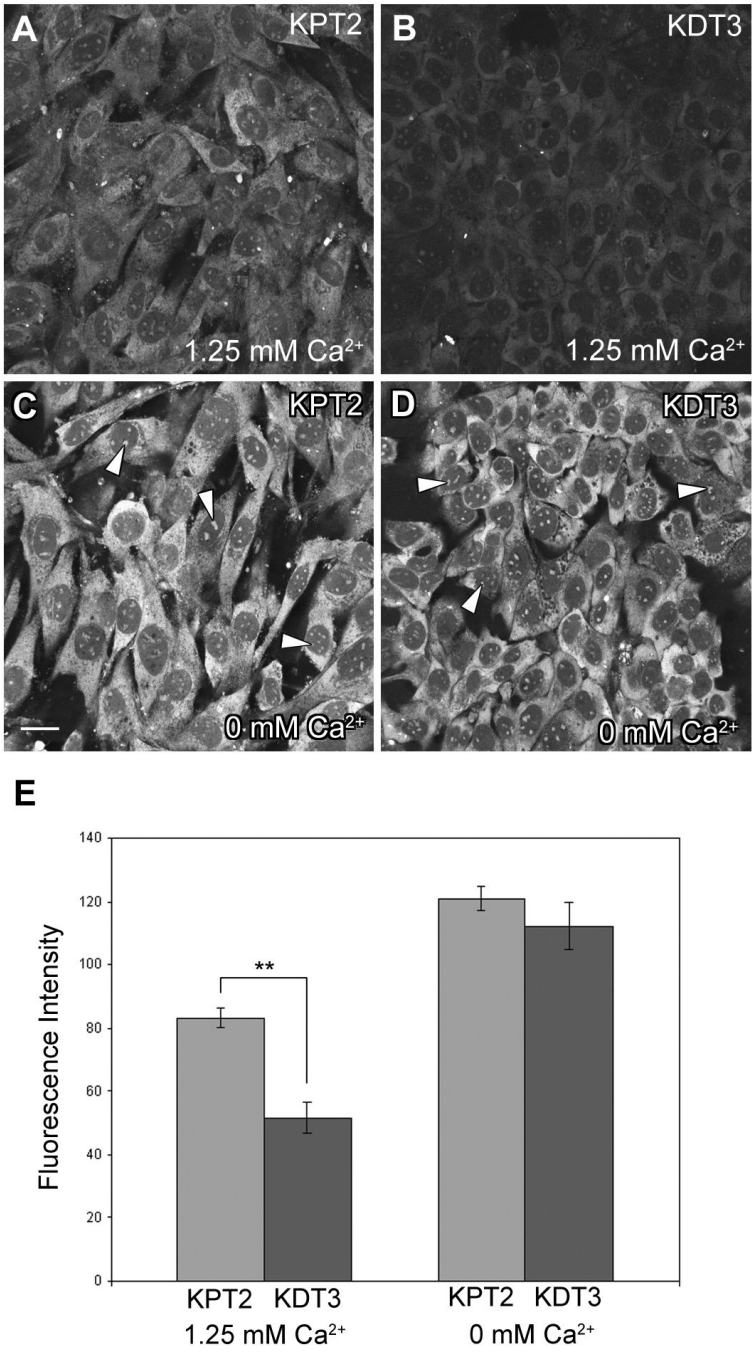


**Fig. 3.**

GTTR uptake is enhanced in the absence of extracellular $Ca^{2+}$. In the presence of extracellular 1.25 mM $Ca^{2+}$, KPT2 and KDT3 cells had modest and low levels of intracellular GTTR fluorescence, respectively, after 30 seconds of GTTR treatment (A,B). In the absence of extracellular $Ca^{2+}$, KPT2 cells had a modest increase in GTTR fluorescence (C), while KDT3 cells had substantially enhanced GTTR uptake (D). In both KPT2 and KDT3 cells, GTTR fluorescence was diffusely distributed in the cytoplasm, with small puncta (arrowheads) within the nucleus. (E) Fluorescence intensity of cytoplasmic GTTR in KDT3 cells was significantly lower than in KPT2 cells in the presence of extracellular $Ca^{2+}$ (**$p$<0.01). Removal of extracellular $Ca^{2+}$ greatly enhanced GTTR fluorescence in both

KPT2 and KDT3 cells compared to 1.25 mM $Ca^{2+}$ condition ($p<0.001$). The enhanced GTTR levels by extracellular $Ca^{2+}$ removal were similar between KPT2 and KDT3 cells. Fluorescence intensity data are shown as mean ± s.d. Bar, 20 μm.

NIH-PA Author Manuscript
NIH-PA Author Manuscript
NIH-PA Author Manuscript

NIH-PA Author Manuscript
NIH-PA Author Manuscript
NIH-PA Author Manuscript



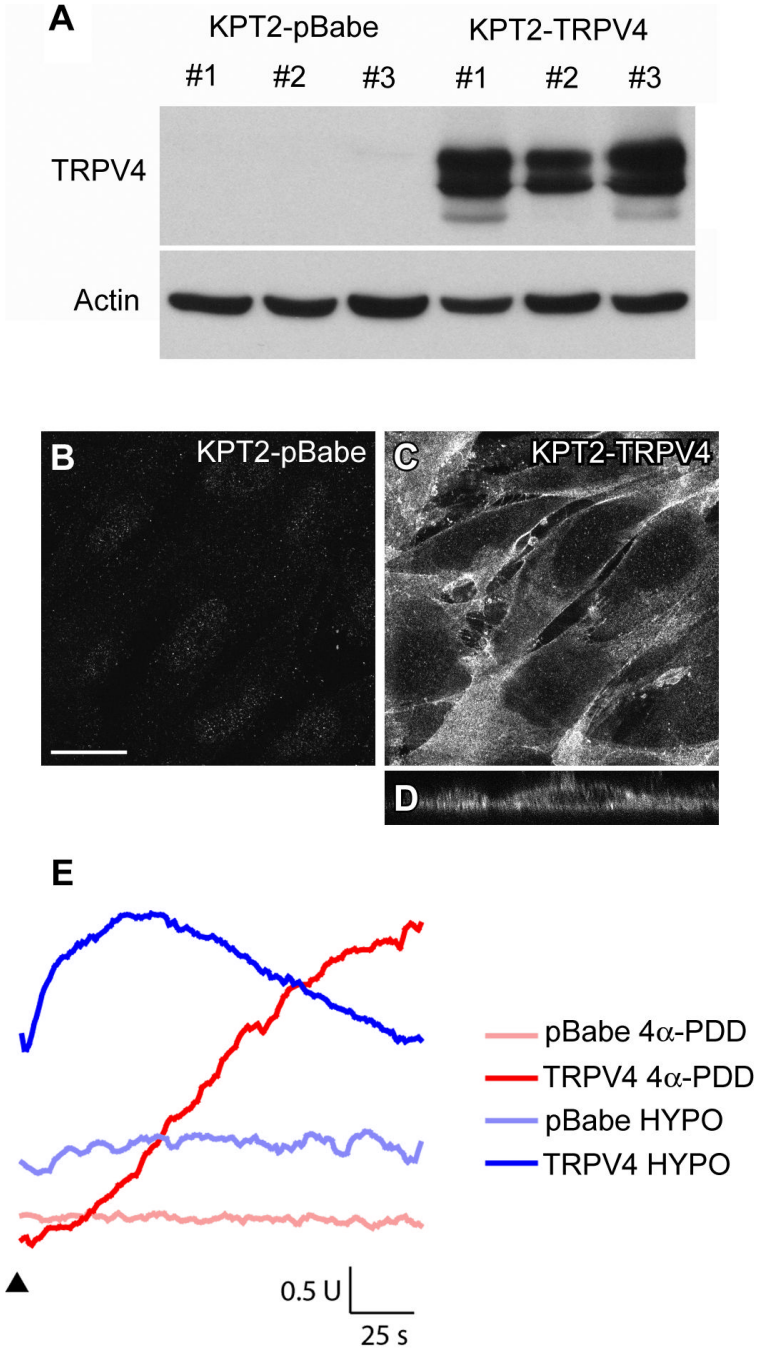


**Fig. 4.**

Generation of KPT2-derived cell lines that express TRPV4. (A) In immunoblots, three empty vector control clones (KPT2-pBabe) did not express TRPV4, while three TRPV4-expressing clones (KPT2-TRPV4) highly expressed TRPV4 with two or three bands around 110 kDa. Actin levels at 42 kDa confirmed that there were similar amounts of total proteins in the samples. There was negligible TRPV4 expression in KPT2-pBabe cells (B). In KPT2-TRPV4 cells, immunofluorescence showed uniform localization of TRPV4 at the cell membrane (C). Orthogonal view of KPT2-TRPV4 shows that TRPV4 protein expression is uniform in the membrane, including the apical membrane (D). Bar in B also applies for C and D (20 μm). TRPV4-dependent $Ca^{2+}$ entry in response to hypotonic stress or the TRPV4

agonist α-PDD was observed in KPT2-TRPV4 cells, but not in KPT2-pBabe cells (E). Fura-2 fluorescence was monitored as an index of intracellular $Ca^{2+}$ concentration (see Materials and Methods), and the fura-2 ratio (in arbitrary unit; U) is depicted as a function of time. Arrowhead denotes onset of hypotonic stress or addition of 4α-PDD.

NIH-PA Author Manuscript
NIH-PA Author Manuscript
NIH-PA Author Manuscript

NIH-PA Author Manuscript
NIH-PA Author Manuscript
NIH-PA Author Manuscript



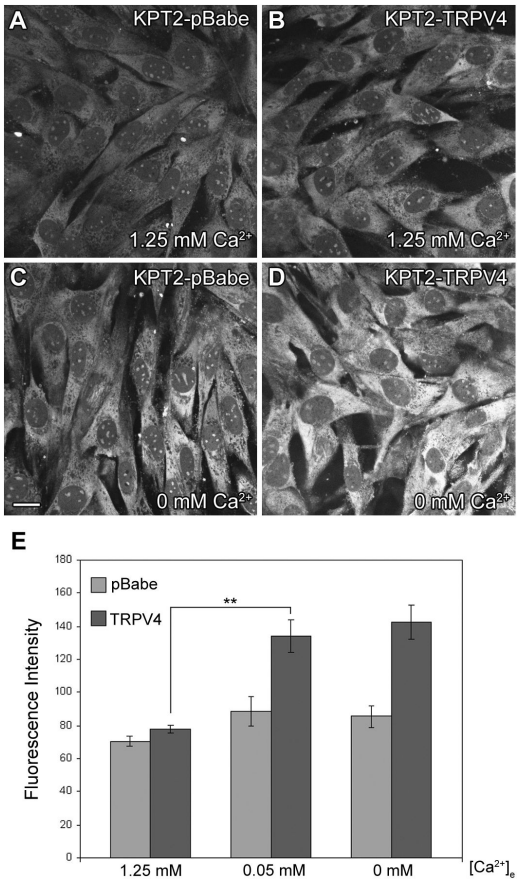


**Fig. 5.**

KPT2-TRPV4 cell lines show enhanced GTTR uptake in the absence of extracellular $Ca^{2+}$. After 30 seconds of GTTR treatment, there was little difference in GTTR uptake between KPT2-TRPV4 and KPT2-pBabe cells in the presence of extracellular $Ca^{2+}$ (A,B), with no significant difference in fluorescence intensity of cytoplasmic GTTR (E). Enhanced GTTR uptake was observed in KPT2-TRPV4 cells in the absence of extracellular $Ca^{2+}$ compared to KPT2-pBabe cells (C,D). Similar results were obtained for all the three KPT2-TRPV4 and three KPT2-pBabe cell lines. Fluorescence intensity of cytoplasmic GTTR in KPT2-TRPV4 cells was significantly higher than KPT2-pBabe cells in 0 or 0.05 mM extracellular $Ca^{2+}$ condition (E). Fluorescence intensity data are shown as mean ± s.d. $^{**}p<0.01$. Bar in C also applies for A, B, and D (20 μm).

NIH-PA Author Manuscript

NIH-PA Author Manuscript

NIH-PA Author Manuscript

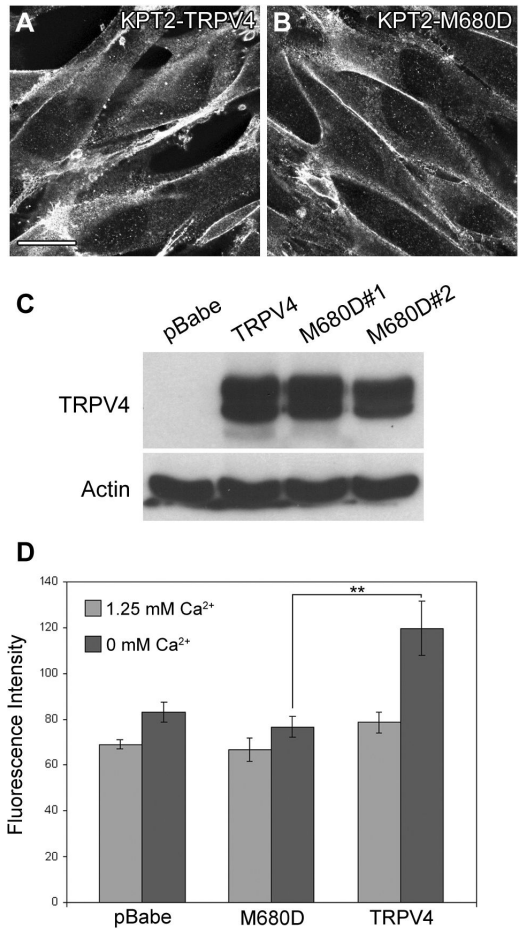


**Fig. 6.**

GTTR uptake by TRPV4 is dependent on M680 residue within the channel pore. KPT2-derived cell lines that express M680D mutant of TRPV4 (KPT2-M680D) were generated and tested for GTTR uptake. Immunofluorescence confirmed M680D mutant had normal membrane localization in the cells (A,B). Immunoblotting showed similar protein expression levels of TRPV4 wild-type and M680D mutant in KPT2-TRPV4 and two clones of KPT2-M680D (M680D#1 and #2), respectively (C). After 30 seconds of GTTR treatment, there was no significant enhancement in GTTR uptake by extracellular $Ca^{2+}$ removal in KPT2-M680D cells, and similar results were obtained for the two KPT2-M680D cell lines (D). Fluorescence intensity data are shown as mean ± s.d. $^{**}p<0.01$. Bar in A also applies for B (20 μm).

NIH-PA Author Manuscript
NIH-PA Author Manuscript
NIH-PA Author Manuscript



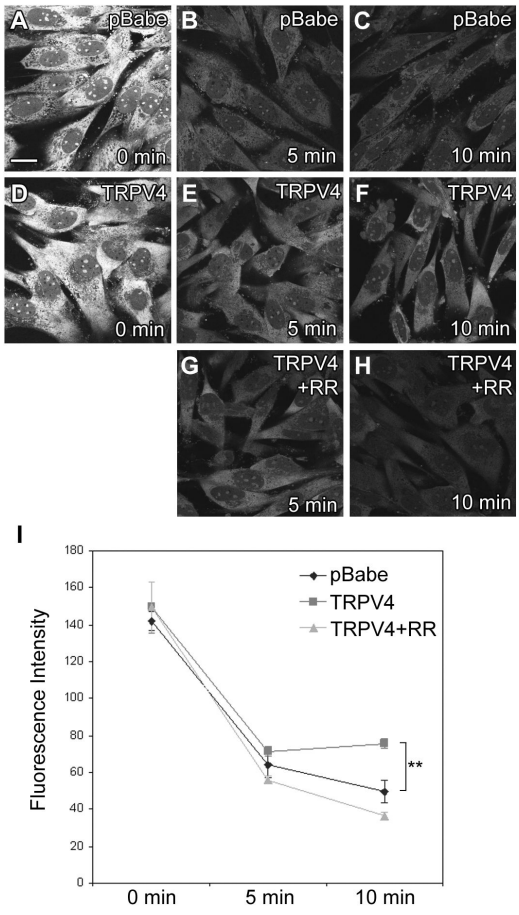


**Fig. 7.**

TRPV4 contributes to GTTR retention in KPT2-TRPV4 cells in an endolymph-like extracellular environment. After 1 minute of GTTR treatment in PBS with $Ca^{2+}$ at 1.25 mM, KPT2-pBabe and KPT2-TRPV4 cells had similar levels of GTTR (A,D). After incubation in the clearance buffer, KPT2-pBabe cells had lower GTTR fluorescence levels compared to KPT2-TRPV4 cells (B,C,E,F). Treatment with 10 μM RR to block inward currents accelerated GTTR clearance from KPT2-TRPV4 cells (G,H). Fluorescence intensity of cytoplasmic GTTR was quantified and statistically analyzed, and data are shown as mean ± s.d. (I). $^{**}p<0.01$. Bar in A also applies for B-H (20 μm).